Case Study of Data Assimilation Methods with the LWR–Proteus Phase II Experimental Campaign

Conference Paper · April 2017

4 authors:

Daniel Siefman
École Polytechnique Fédérale de Lausanne
13 PUBLICATIONS **7** CITATIONS
SEE PROFILE

Mathieu Hursin
Paul Scherrer Institut
42 PUBLICATIONS **100** CITATIONS
SEE PROFILE

Peter Grimm
Paul Scherrer Institut
44 PUBLICATIONS **265** CITATIONS
SEE PROFILE

Andreas Pautz
École Polytechnique Fédérale de Lausanne
104 PUBLICATIONS **206** CITATIONS
SEE PROFILE

Some of the authors of this publication are also working on these related projects:

Project COLIBRI View project

Project BUCSS-R View project

Case Study of Data Assimilation Methods with the LWR-Proteus Phase II Experimental Campaign

Daniel J. Siefman[*][†], Mathieu Hursin[*][†], Peter Grimm[†], Andreas Pautz[*]

[*]*Laboratory for Reactor Physics and Systems Behavior, EPFL, Lausanne, Switzerland*
[†] *Experimental Reactor Physics, PSI, Villigen, Switzerland*
daniel.siefman@epfl.ch, mathieu.hursin@psi.ch, peter.grimm@psi.ch, andreas.pautz@epfl.ch

Abstract - *This paper describes the application of data assimilation methods to CASMO-5 simulations of a Proteus research reactor experiment. Its focus is a comparison and evaluation of three prominent data assimilation methods: generalized linear least squares, MOCABA, and Bayesian Monte Carlo. These methods have not yet been extensively compared to date. The experiment is an interesting case study for this comparison because the measured reactivity worth response can be non-linear. This study investigates the effects that non-linearity has upon the agreement between the methods. The adjusted calculated values, calculation uncertainty, and nuclear data are all investigated to compare and evaluate the methods. The presented results provide evidence supporting the hypothesis that for linear responses, all of the data assimilation methods agree well. But when the responses become more non-linear, significant disagreements occur between generalized linear least squares results and those of MOCABA and Bayesian Monte Carlo.*

I. INTRODUCTION

Many institutes have, in a worldwide effort, developed methods called data assimilation (DA). These methods tackle biases and uncertainties created by input nuclear data (e.g. cross sections, fission multiplicity) in neutronics simulations [1]. They identify important nuclide/reaction pairs and associated energy ranges which contribute largely to calculation bias and uncertainty and seek to ameliorate the bias and to reduce that calculation uncertainty. Additionally, DA can be used to give recommendations to nuclear data evaluators to aid in improving their evaluations. Three methods for DA have gained prominence in the field of neutronics: Generalized Linear Least Squares (GLLS) [2], MOCABA [3], and Bayesian Monte Carlo (BMC) [4],[5]. Each method has its advantages and disadvantages that, to date, have not been extensively investigated in a comparative sense. Such a comparison would help to determine in which cases a method is superior, deficient, or equal to another in their effectiveness as a DA tool.

The present paper is a case study seeking to perform this comparison with the LWR Phase II (LWR-PII) experimental campaign of the research reactor Proteus at the Paul Scherrer Institute [6]. In this campaign, the reactivity worth of several spent fuel segments was measured by introducing them into a mock-up of a fresh PWR assembly. The fuel samples were cut from UO_2 and MOX fuel rods irradiated in Swiss nuclear power plants to burnups ranging between 20 and 120 MWd/kg. This study calculates reactivity effects using CASMO-5 [7] and then uses the sensitivity analysis and uncertainty quantification tool SHARK-X [8] to compute parameters for DA. The project's long-term goal is to apply DA with LWR-PII to safety analyses of a Swiss nuclear power plant's spent fuel pool.

LWR-PII is an interesting case study because the main measured response, relative reactivity worth, is non-linear. This may cause it to exceed the linearity assumption used in GLLS. MOCABA and BMC are based on stochastic sampling and are, therefore, global methods and not limited by the response's order. LWR-PII was specially chosen as a case study to investigate and compare these DA methods because of this non-linearity. The DA methods are applied to two sets of integral parameters that are identical, in terms of CASMO-5 modeling, in all ways except for the type of moderator used in Proteus' configuration. The first moderator is water with ~2,000 ppm of boric acid. These responses have a strong degree of linearity and serve as a control to test the agreement of the DA methods for a linear case. The second moderator is pure water that creates more non-linear responses. The results are used as evidence to assess the hypothesis that non-linearity can significantly affect the results of GLLS.

In this paper, results and conclusions are presented concerning the effectiveness of each method when applied with CASMO-5 to LWR-PII. Conclusions are drawn based on adjustments to the CASMO-5 calculated values and reductions of their uncertainty as well as on adjustments to input nuclear data and their uncertainties. Unavoidable biases exist in the nuclear data adjustments because the resonance self-shielding treatment in CASMO is not fully taken into account when nuclear data are perturbed in SHARK-X. Additionally, the prediction of leakage changes by the 2D reflected assembly model used in CASMO may not be totally realistic and introduce biases into the adjustments. Therefore, the adjustments to nuclear data are only interpreted qualitatively.

The paper is organized to first give a theoretical introduction to the three DA methods. Then a summary of the LWR-PII experiment is presented along with a description of the methods used to analyze the experiment. Next, the application of the DA methods to the two experimental sets of integral parameters is presented. The DA results of each set of integral parameters using the methods are compared and used to evaluate the methods and search for effects of non-linearity.

II. THEORY

DA works by using integral experiments to adjust calculated values and input nuclear data. These adjustments are done so that calculated values better agree with their experi-

mental counterparts. The adjusted calculated values and nuclear data are called *posteriors*. DA is subdivided in this paper into deterministic and stochastic methods. GLLS is categorized as deterministic and MOCABA and BMC as stochastic. GLLS requires sensitivity coefficients; the method by which to create them depends upon the neutron transport code used and the type of integral parameter. MOCABA and BMC require random sampling of the nuclear data using their variance-covariance information to create a sample set of responses.

1. Generalized Linear Least Squares (GLLS)

The GLLS technique [2] is widely used by many institutions (JAEA, ORNL, CEA, INL [1]) in their DA packages. GLLS is, in simple terms, a form of regression analysis used to predict adjustments to nuclear data, σ, that would create the best agreement between measured values, E, and calculated values, C, for integral parameters. The assumption is then made that C would be equal to E if not for nuclear data and experimental uncertainties. C is considered a function, $C(\sigma)$, that relates the selected nuclear data's influence on integral parameters. This function is assumed to be represented by a generalized linear model, Eq. (1). This can also be thought of as a first-order Taylor series approximation performed on $C(\sigma)$, with the sensitivity coefficients, S, being the first derivatives. The variable σ is a vector containing the nuclear data with a size ($N_\sigma \times 1$) equal to the number of isotope/reaction pairs × number of energy groups in the nuclear data. S is a matrix of dimensions $N_E \times N_\sigma$, where N_E is the number of integral parameters considered. $C(\sigma)$ is a vector of size $N_E \times 1$.

$$C(\sigma) \approx C(\sigma_0) + S(\sigma - \sigma_0) \tag{1}$$

$C(\sigma)$ is then fit to E (size: $N_E \times 1$) using the least squares method, i.e., by minimizing the error between E and $C(\sigma)$. This fitting gives the posterior mean values of the nuclear data, σ', and their variance-covariance matrix (VCM) M'_σ as shown in Eq. (2) and Eq. (3) respectively. Here M_E and M_σ are the VCMs of the experimental parameters (size: $N_E \times N_E$) and the nuclear data (size: $N_\sigma \times N_\sigma$).

$$\sigma' = \sigma + M_\sigma S^T [SM_\sigma S^T + M_E]^{-1}[E - C(\sigma)] \tag{2}$$

$$M'_\sigma = M_\sigma - M_\sigma S^T [SM_\sigma S^T + M_E]^{-1} SM_\sigma \tag{3}$$

The posterior calculated value, C', is then given by plugging in σ' into Eq. (1) as σ, with σ_0 being the prior nuclear data. This is shown in Eq. (4). The posterior VCM of C, M'_C, can then be calculated with S and M'_σ using Eq. (5), commonly called the *sandwich rule*.

$$C'(\sigma') \approx C(\sigma_0) + S(\sigma' - \sigma_0) \tag{4}$$

$$M'_C = SM'_\sigma S^T \tag{5}$$

2. MOCABA

Recent research at Areva has led to the MOCABA framework for DA [3]. MOCABA was developed as an alternative to the GLLS methodology. MOCABA seeks to avoid GLLS' technical limitations linked to first-order perturbation theory and to be applicable in cases where adjoint-based first-order perturbation theory is unavailable. MOCABA avoids both of these limitations by using the Monte Carlo method to perform Bayesian inference. MOCABA was shown in [3] to be a non-perturbative form of GLLS or, in other words, the GLLS equations are linear estimates of MOCABA equations.

MOCABA's method begins with Bayes' theory where calculated values, C, have a prior distribution $p(C)$. The distribution $p(C)$ represents the knowledge of C before the Bayesian update, or before DA. Additionally, $p(C)$ is assumed to have a multivariate normal distribution with means C_0 and a VCM M_C (size: $N_E \times N_E$). The experimental values, E, are the evidence used to update the prior. The Bayesian update gives the posterior $p(C|E)$, with updated moments for the multivariate normal distribution of C: C' and M'_C. The formulas for calculating C' and M'_C are given in Eqs. (6) and (7). The posterior nuclear data's mean values and VCM are given by Eqs. (8) and (9), where $M_{\sigma,C}$ (size: $N_\sigma \times N_E$) is the covariance matrix between C and σ.

MOCABA DA uses the Monte Carlo method to randomly sample nuclear data with the uncertainty information found in VCM files. For every randomly sampled nuclear data file, σ_i, a simulation is performed to create a calculated value $C_i(\sigma_i)$. If N samples of σ are done, N simulations are then performed creating a population of calculated values: $C_1(\sigma_1)$, $C_2(\sigma_2)$, ... , $C_n(\sigma_n)$. This population set is then used to estimate $p(C)$, or more specifically C_0 and M_C. A covariance matrix, $M_{\sigma,C}$, is also calculated from the population sets and estimates the covariance between C and σ. Eqs. (6) and (7) can then be applied to calculate C' and M'_C. $M_{\sigma,C}$ is used in Eqs. (8) and (9) to get σ' and M'_σ.

$$C' = C + M_C(M_C + M_E)^{-1}(E - C) \tag{6}$$

$$M'_C = M_C - M_C(M_C + M_E)^{-1}M_C^T \tag{7}$$

$$\sigma' = \sigma + M_{\sigma,C}(M_C + M_E)^{-1}(E - C) \tag{8}$$

$$M'_\sigma = M_\sigma - M_{\sigma,C}(M_C + M_E)^{-1}M_{\sigma,C}^T \tag{9}$$

3. Bayesian Monte Carlo (BMC)

BMC [4] [5] uses Bayes' theorem to get C', M'_C, σ', and M'_σ. Bayes' theorem for DA is shown in Eq. (10) with the prior distribution $p(\sigma)$ and likelihood function $L(\sigma|E)$ being used to get a posterior distribution for nuclear data $p(\sigma'|E)$.

$$p(\sigma'|E) \propto L(E|\sigma)p(\sigma) \tag{10}$$

The Bayesian update is performed by estimating a maximum of $L(\sigma|E)$ by randomly sampling $p(\sigma)$ to get a sample set of C_i vectors, with the VCM M_C estimated from the population set. These C_i values are compared to E to find which

randomly sampled σ_i creates the best agreement between C and E, i.e. maximizes the likelihood of getting these experimental/calculated values given the assumptions for the prior distribution.

The likelihood function for a σ_i is given by Eq. (11). Here χ_i^2 is the χ^2-distribution as calculated in Eq. (12).

$$L(E|\sigma_i) \propto e^{-\chi_i^2/2} \tag{11}$$

$$\chi_i^2 = (E - C_i(\sigma_i))^T M_E^{-1} (E - C_i(\sigma_i)) \tag{12}$$

Each χ_i^2 from a random sampling of the nuclear data is used to calculate a weight for that sample set, w_i. Sample sets with higher w_i contribute more to adjusting $p(\sigma)$, where sample sets with lower w_i contribute less. The weight of σ_i is given in Eq. (13), where $L(\sigma_0|E)$ is the likelihood function of the zeroth sample set, or the unperturbed σ. Smaller χ_i^2 values, or better agreement between E and $C_i(\sigma_i)$, create larger weights.

$$w_i = \frac{L(E|\sigma_i)}{L(E|\sigma_0)} \tag{13}$$

The weights are then used to calculate posterior moments for C and σ seen in Eq. (14) and Eq. (15) for C' and M_C' and in Eq. (16) and Eq. (17) for σ' and M_σ'.

$$C' = \frac{\sum_{i=1}^{N} w_i \times C_i(\sigma_i)}{\sum_{i=1}^{N} w_i} \tag{14}$$

$$M_C' = \frac{\sum_{i=1}^{N} w_i \times (C_i(\sigma_i) - C_i(\sigma_0))^T (C_i(\sigma_i) - C_i(\sigma_0))}{\sum_{i=1}^{N} w_i} \tag{15}$$

$$\sigma' = \frac{\sum_{i=1}^{N} w_i \times \sigma_i}{\sum_{i=1}^{N} w_i} \tag{16}$$

$$M_\sigma' = \frac{\sum_{i=1}^{N} w_i \times (\sigma_i - \sigma_0)^T (\sigma_i - \sigma_0)}{\sum_{i=1}^{N} w_i} \tag{17}$$

III. EXPERIMENT DESCRIPTION AND INPUT PARAMETERS

In each LWR-PII measurement, the absolute reactivity worth, $\Delta\rho$, of an irradiated fuel rod taken from a Swiss nuclear power plant was measured. $\Delta\rho$ was evaluated as the change in k_{eff} created by replacing a reference sample (U_{ref}) of fresh, 3.5 w.% enriched UO_2 with the irradiated fuel sample. $\Delta\rho$ was then calculated with with Eq. 18. In addition, $\Delta\rho$ of a natural uranium sample (U_{nat}) instead of the irradiated fuel was also evaluated with this method. This $\Delta\rho$ with U_{nat} was then used to create a ratio of reactivity worths called *relative reactivity worth* as seen in Eq. 19. $\Delta\rho_{rel}$ was used and not $\Delta\rho$ so that accurate comparisons can be made between CASMO calculated values and experimental values. This is because, unlike $\Delta\rho$, $\Delta\rho_{rel}$ is independent of the size of the system calculated. It can therefore be used in a CASMO model where only a sub-system of the core is simulated in 2D [6].

$$\Delta\rho = \frac{1}{k_{ref}} - \frac{1}{k_{sample}} \tag{18}$$

$$\Delta\rho_{rel} = \frac{\Delta\rho(U_{ref} \to sample)}{\Delta\rho(U_{ref} \to U_{nat})} \tag{19}$$

This analysis performs DA on three sets of integral parameters. During LWR-PII, each set of integral parameters was measured with a different moderating condition at atmospheric temperature and pressure in the reactor's center assembly. The moderating conditions investigated in the experiment were full-density H_2O, a mixture of H_2O and D_2O (37.0 w% D_2O), and borated H_2O ($\sim$2,000 ppm of boric acid). In this paper, only results for the borated moderating condition (henceforth called BHO) and the full-density H_2O moderator are presented. These moderators will be most useful in the future when DA will be applied to analyzing a spent fuel pool. Additionally, the contrast between the results of BHO and H_2O moderators highlights differences that can occur between deterministic and stochastic DA methods when non-linearities are present. The calculated $\Delta\rho_{rel}$ responses behave more non-linearly with the H_2O moderator than the BHO moderator. To ease the analysis in this study, the experimental values are assumed to have an uncertainty of 1.5% and to be fully uncorrelated.

In this analysis, the uncertainty associated with nuclear data of 41 isotopes is investigated using the SCALE6.1 VCM [9] and the stochastic sampling (SS) and equivalent generalized perturbation theory (EGPT) modules in SHARK-X [8]. SS is used to randomly sample the nuclear data and create the sample set of calculated responses for stochastic DA. EGPT is used to calculate the sensitivity coefficients for GLLS. According to the EGPT approach, the sensitivity coefficient of $\Delta\rho_{rel}$ can be expressed as a function of the k-sensitivity coefficients of the reference and two perturbed states, as seen in Eq. 20. Here, $S_{k_{ref},\sigma}$, $S_{k_1,\sigma}$, and $S_{k_2,\sigma}$ are the sensitivity coefficients of k_{eff} for the reference state and perturbed states 1 and 2. The variables λ_{ref}, λ_1, and λ_2 are the states' lambda eigenvalues as calculated by CASMO-5. For $\Delta\rho_{rel}$, state 1 is a given fuel sample, and state 2 is the natural fuel sample.

$$S_{\Delta\rho_{rel},\sigma} = -\frac{\lambda_{ref}(\lambda_1 - \lambda_2)}{(\lambda_{ref} - \lambda_1)(\lambda_{ref} - \lambda_2)} S_{k_{ref},\sigma}$$
$$+ \frac{\lambda_1}{\lambda_{ref} - \lambda_1} S_{k_1,\sigma} - \frac{\lambda_2}{\lambda_{ref} - \lambda_2} S_{k_2,\sigma} \tag{20}$$

For low atomic number nuclides (e.g. H, O, Zr, Nd) only the total scattering and total capture cross sections are considered: no distinction was made between inelastic and elastic scattering. The following reactions were considered for fissile and fertile nuclides: elastic scattering (σ_e), inelastic scattering (σ_i), (n,2n) reaction, fission (σ_f), capture (σ_c), average number of neutrons per fission ($\bar{\nu}$), and fission spectrum (χ). The CASMO-5 neutron transport simulations, the nuclear data, and sensitivity coefficients are all obtained in CASMO-5's 19-energy-group structure.

Sample & Burnup [MWd/kg]	R^2	Prior C/E	Posterior Bias C'/E			Prior 1 Rel. Std. [%]		Posterior 1 Rel. Std. [%]		
			GLLS	MOCABA	BMC	EGPT	SS ± Conf. Int	GLLS	MOCABA	BMC
U1* (~40)	0.976	0.950	0.943	0.943	0.943	1.79	1.76 ± 0.07	0.43	0.40	0.41
U2 (~50)	0.976	1.016	1.011	1.011	1.010	1.15	1.13 ± 0.05	0.39	0.30	0.31
U3 (~70)	0.983	0.980	0.975	0.976	0.975	1.03	1.01 ± 0.04	0.38	0.31	0.32
U5 (~90)	0.982	1.004	1.000	1.000	1.000	0.97	0.96 ± 0.04	0.40	0.32	0.33
U6 (~90)	0.995	0.991	0.987	0.987	0.987	0.98	0.95 ± 0.04	0.41	0.32	0.33
U7 (~120)	0.994	0.997	0.993	0.993	0.992	1.04	1.02 ± 0.05	0.46	0.37	0.37
UO$_2$ mean	0.984	0.990	0.985	0.985	0.985	1.16	1.14 ± 0.05	0.41	0.34	0.35
M1 (~20)	0.996	1.035	0.999	0.998	0.997	8.13	8.09 ± 0.36	1.09	1.39	1.35
M2* (~40)	0.991	1.053	1.035	1.033	1.032	3.91	3.88 ± 0.17	0.71	0.70	0.67
M3 (~60)	0.992	1.018	1.007	1.005	1.004	2.49	2.48 ± 0.11	0.65	0.59	0.58
M4 (~70)	0.935	1.034	1.024	1.022	1.022	2.11	2.09 ± 0.09	0.64	0.56	0.56
MOX mean	0.979	1.035	1.016	1.014	1.014	4.16	4.14 ± 0.18	0.77	0.81	0.79

TABLE I. Prior and posterior biases and 1-relative-standard deviations using each DA method. An asterisk (*) indicates removal from influencing the adjustments by $\Delta\chi^2$-filtering. Sample U4 is missing because it was not experimentally measured for BHO.

IV. RESULTS AND ANALYSIS

The results of the data assimilation for the BHO and H$_2$O moderating conditions are presented separately in the following sections. First, for a given moderator, the methods' ability to improve the calculation bias and reduce the calculation uncertainty are presented and analyzed. Then a summary of the analyzed adjustments to nuclear data is presented. The data assimilation for the BHO-moderated integral parameters is presented first to test the hypothesis that the DA methods agree well for linear integral parameters. Next, the more non-linear, H$_2$O-moderated responses are examined to test the hypothesis that heightened discrepancies will be seen between GLLS and MOCABA/BMC results with non-linearities present.

The degree of linearity of a response is assessed by calculating a coefficient of determination, or R^2. In the context of this study, R^2 is the square of the correlation between a response's values and the best predictions that can be computed from a linear approximation of the dependence of a response on the nuclear data. R^2 takes values between 0 and 1. Higher values of R^2 indicate better predictability of the response using the assumed linear approximation. R^2 is calculated in this analysis by using the N randomly sampled nuclear data sets and the sensitivity coefficients produced by SHARK-X. Eq. 21 is used to calculate R^2 where σ_i is a randomly sampled nuclear data set, $C(\sigma_i)$ is the response calculated by CASMO when σ_i is used as input, $C_s(\sigma_i)$ is the calculated response using Eq. 1 with σ_i and the response's sensitivity coefficients, and $C(\sigma_0)$ is the calculated response with CASMO using the unperturbed nuclear data, σ_0.

$$R^2 = 1 - \frac{\sum_{i=1}^{N}\left(C(\sigma_i) - C_s(\sigma_i)\right)^2}{\sum_{i=1}^{N}\left(C(\sigma_i) - C(\sigma_0)\right)^2} \qquad (21)$$

1. BHO: Adjustments to Calculated Values

The prior and posterior calculated-to-experimental (C/E) ratios for $\Delta\rho_{rel}$ and the relative standard deviations of these values are compared in Table I, where they are arranged by increasing burnup and by fuel type. The uncertainties given in Table I include only contributions from nuclear data and are obtained with either EGPT or SS as described in Section III. The uncertainties from SS include their 95% confidence intervals [10] and show that the differences in the prior uncertainties between EGPT and SS are not statistically significant. Additionally, the R^2 values are shown for each response as calculated with Eq. 21. Samples U1 and M2 were removed from the data assimilation by $\Delta\chi^2$-filtering [11]. This method removes responses from the adjustment procedure if their χ^2 value exceeds 3.0. Responses are removed because the disagreement between C and E is too large to be explained by nuclear data and experimental uncertainties. With too high χ^2 values, the DA theories' assumptions are violated and these integral parameters would negatively affect the quality of posteriors.

The adjustment shows good agreement for the posterior C/E values (C'/E) of the methods. The C'/E values never differ by greater than 0.2%, which is less than their 1-relative-standard deviations. The adjustments to the UO$_2$ samples show a degradation in the agreement between C and E, with the mean C/E decreasing away from 1.0 by 0.3-0.5%. The MOX samples, in contrast, show a 1.2-2.1% decrease in C/E moving closer to the desired values of 1.0. The UO$_2$ samples likely show poorer adjustments because the MOX samples dominate the DA as they have higher prior biases and uncertainties. The good agreement between the methods indicates, first, the consistency in their formulations. Second, it shows that despite some non-linearity for these responses with average R^2 values of 0.984 for UO$_2$ and 0.979 for MOX samples, these degrees of non-linearity did not significantly invalidate GLLS' linearity assumption and cause significant discrepancies in the results.

Examining the reduction in C'/E uncertainties in the form of relative standard deviations, good agreement is seen between methods, especially between MOCABA and BMC. For these two stochastic methods, the differences between C uncertainties are less than 0.01%, except for M1 and M2 which are approximately 0.04% and 0.03% respectively. Larger disagreements are seen between GLLS and the two stochastic methods. The most significant discrepancy is seen for sample M1, where the MOCABA and BMC uncertainties are 0.30% and 0.26% larger than GLLS', respectively. The results support this study's hypothesis: MOCABA and BMC should agree very well and, with a slight non-linearity, some small differences between the stochastic methods and GLLS should be seen.

One difficulty in comparing MOCABA and BMC's results to GLLS' is created by the finite sample size of the randomly sampled nuclear data and, therefore, the sampled $\Delta\rho_{rel}$ values. This means that the moments of a $\Delta\rho_{rel}$ value's prior distribution (in particular its mean and variance or, C_0 and M_C) are only approximations and not the moments of the true population or, in other words, the sample set if its size was infinite. The consequence of this fact is that the inputs into, for instance, MOCABA's equations would vary from one sample size of 1,000 to another, potentially creating the discrepancies between MOCABA/BMC and GLLS seen in Table I. These disagreements from statistical fluctuations could be erroneously attributed to linearity effects and lead to type I or type II errors when evaluating the paper's working hypothesis. Type I errors occur when the hypothesis would be erroneously declared false when it is in fact true. Type II errors occur when the hypothesis would be erroneously declared true when it is in fact false. With the current hypothesis that "if the integral parameters are linear then the DA methods give equivalent results," a type I error would occur when concluding from the evidence that the DA methods do not agree when they in fact do. A type II error would be concluding from the evidence that they do agree when they in fact do not.

A very large sample size is needed to investigate the effects of statistical uncertainties in the prior distributions' moments on the MOCABA and BMC methods' results. A large sample size is, however, difficult to create because of the high computational costs required by the large number of CASMO-5 simulations it would need. To create a large sample size and not suffer from high computational costs, a metamodel was used to create 1 million samples for each $\Delta\rho_{rel}$ response. The 1 million samples were grouped into 1,000 sets of 1,000 samples and then used in the MOCABA and BMC methods. This practically means that 1,000 prior distributions were calculated (i.e. 1,000 C_0 and 1,000 M_C) each from 1,000 independent response samples and used to calculate 1,000 posterior distributions. These results would then approximate the fluctuations in the posterior distributions that would be created by fluctuations in the prior distributions due to the finite sample size used in the results presented in Table I.

The metamodel was made by using the k_{eff} sensitivity coefficients of the fuel samples, 1 million random samples of the nuclear data, and the linear approximation used in GLLS' methodology described previously in Eq. 1. This equation is reformulated below as Eq. 22. The k_{eff} sensitivity coefficients,

$S_{k_{eff}}$, and each perturbed nuclear data set, σ_i, are plugged into Eq. 22 to calculate k_{eff} values for each of the 11 fuel samples and the reference and naturally enriched fuel samples. These k_{eff} values are then used in Eq. 18 and Eq. 19 to calculate $\Delta\rho_{rel}$. With the 1 million random samples of the nuclear data, 1 million k_{eff} values are calculated which are then used to calculate 1 million $\Delta\rho_{rel}$ values. These 1 million $\Delta\rho_{rel}$ values are split into 1,000 sets of 1,000 values, whose means and VCMs are then used by MOCABA and BMC. Because the k_{eff} values are highly linear ($R^2 > 0.99$), this metamodel is considered to be sufficiently accurate to capture the statistical behavior of a true large sample set of $\Delta\rho_{rel}$. The linearity of k_{eff} values means that for a given set of nuclear data, the k_{eff} calculated with CASMO-5 using this nuclear data and with the Eq. 22 agree very well.

$$k_{eff}^{(i)}(\sigma_i) \approx k_{eff}(\sigma_0) + S_{k_{eff}}(\sigma_i - \sigma_0) \tag{22}$$

An example of the results of the metamodel analysis for MOCABA is presented graphically in Fig. 1 for C/E and Fig. 2 for the relative standard deviation of C. Included in the plots are the prior values of each sample set of 1,000 for C/E and the relative standard deviation, and the posterior MOCABA values calculated with each sample set's prior distribution. Additionally, the GLLS C'/E values and relative standard deviation calculated with the original, or zeroth, set of nuclear data are presented.
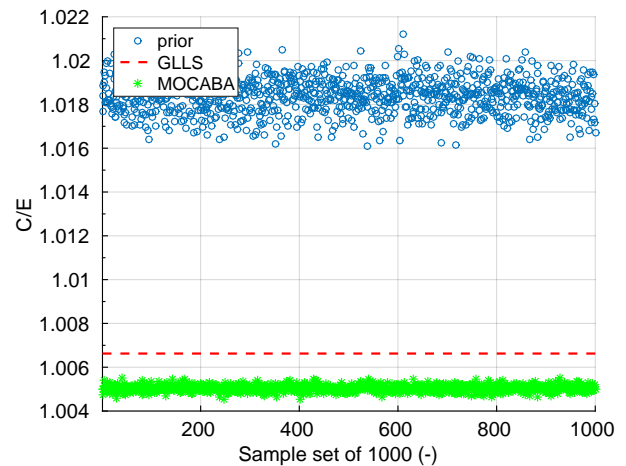

Fig. 1. Distribution of fuel sample M3's prior C/Es and the MOCABA C'/Es with meta-modeling along with the original GLLS C'/E.

Turning first to C/E in Fig. 1, it is apparent that 1) the difference between the GLLS and MOCABA posterior C'/E is likely statistically significant and that 2) the spread of MOCABA C'/E values is smaller than that of the prior C/E values, indicating that the adjustment to C is not highly sensitive to fluctuations in the prior's mean, C_0. Next examining Fig. 2 for fuel sample M3's $\Delta\rho_{rel}$ relative standard deviations, similar behavior to that of C/E is seen. Namely, the difference between the GLLS and MOCABA posterior relative standard deviations is likely statistically significant, i.e. not caused by the finite sample size used to formulate the prior distribu-
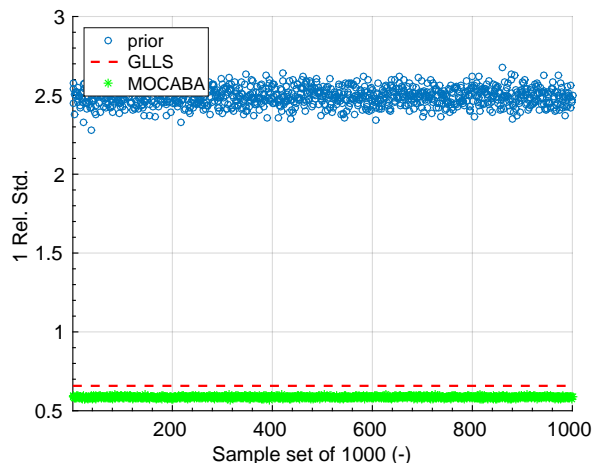
Fig. 2. Distribution of fuel sample M3's prior and MOCABA's 1-relative-standard deviations using metamodeling along with the original GLLS posterior 1-relative-standard deviation.

tion. Additionally the spread of MOCABA's posterior relative standard deviations is smaller than that of the prior's.

The complete results of the metamodeling analysis were analyzed in terms of the standard deviations of the 1,000 sets of prior and posterior distributions' moments. In other words, the results are analyzed in terms of the standard deviation of the sample set of 1,000 C/Es and C'/Es and the standard deviation of the sample set of 1,000 prior and posterior relative standard deviations. This analysis shows that the uncertainty in the posterior C/E (average of 1E-4) is two orders of magnitude smaller than the difference seen between GLLS and MOCABA C'/Es in Table I. Additionally, the uncertainty of the posterior relative standard deviations (the standard deviation of the relative standard deviations) is also, at around 5E-3%, an order of magnitude lower than the discrepancies between MOCABA and GLLS results, which are on the order of 1E-2 to 1E-1%.

The metamodel analysis results for BMC have similar uncertainties to MOCABA for its C'/E values: for all fuel samples, the standard deviations of the C'/Es are approximately 1E-4, thereby indicating that the discrepancies between BMC and GLLS C'/Es are likely statistically significant. A larger uncertainty, by an order of magnitude, is calculated for BMC's posterior relative standard deviations. At approximately 2E-2%, the posterior relative standard deviations' standard deviations are similar to that of the prior relative standard deviations'. Additionally, it is on the same order of magnitude as the discrepancies between the BMC and GLLS posterior relative standard deviations. This means that the differences between BMC and GLLS posterior relative standard deviations may only occur due to statistical fluctuations in the prior distribution.

In conclusion, metamodeling helped show that statistically significant differences exist between GLLS and MOCABA/BMC C'/E values and between the MOCABA and GLLS posterior relative standard deviations. Furthermore, the metamodeling helped confirm that a type I error was not occurring: the null hypothesis that "if the integral parameters

used in DA are linear, then the three DA methods will give equivalent results" was not being incorrectly rejected. Because the responses are not perfectly linear, with average R^2 values of 0.984 and 0.979 for UO_2 and MOX respectively, some discrepancy between GLLS and MOCABA/BMC will be, however, present. Therefore, the results are consistent with the hypothesis but strictly cannot not prove it true. The null hypothesis will be further tested in Section IV.3 when the identical responses become more non-linear with the H_2O moderator.

2. BHO: Adjustments to Nuclear Data

The comparison of each method's ability to adjust nuclear data is summarized here by focusing on the nuclide/reaction pairs that contribute most to uncertainty. The major contributors are $^{239}Pu/\bar{\nu}$, $^{238}U/\sigma_c$, and $^{235}U/\sigma_f$. The adjustments are presented in CASMO-5's 19-energy-group structure in Fig. 3, 4, and 5. Here, the adjustments are shown in the upper figure as relative changes in the nuclear datum from prior to posterior ($\Delta XS/XS$) along with the prior and posterior uncertainties as relative standard deviations in the lower figure.
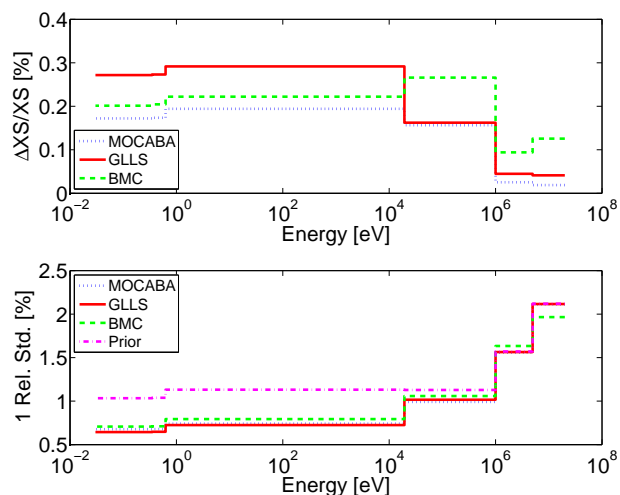

Fig. 3. Adjustments with each DA method to $^{239}Pu/\bar{\nu}$ as $\Delta XS/XS$ (above) and relative standard deviations (below).

First examining Fig. 3, good agreement is seen between all the methods with mean-value adjustments being approximately 0.17%, 0.27%, 0.20% respectively in thermal groups for MOCABA, GLLS, and BMC respectively and 0.19%, 0.23%, and 0.29% respectively in epithermal groups. The reductions in uncertainty are also similar: at the thermal energy range the prior 1-relative-standard-deviation is 1.03% and the posterior MOCABA and GLLS uncertainties are 0.68%, 0.64%, 0.67% for MOCABA, GLLS, and BMC respectively; at the epithermal energy range the prior uncertainty is 1.13% and the posterior uncertainties are 0.74%, 0.72%, 0.74% for MOCABA, GLLS, and BMC respectively.

Examining Fig. 4 for $^{238}U/\sigma_c$, good agreement is seen between MOCABA and GLLS in the thermal energy range where their $\Delta XS/XS$ values are within 0.01% of each other.

BMC predicts a larger increase in the cross section at thermal and epithermal energy ranges by about 0.1-0.2%. Even though BMC adjustments disagree to a greater extent with the other two methods, the adjustments created by the methods all agree within their respective 1-standard-deviation uncertainty intervals. The uncertainty reductions also agree well between the methods, except for BMC at energies at approximately 10^2 - 10^4 eV where BMC's posterior uncertainty increases relative to the prior's. The effects causing this increase in uncertainty are not known at this time.
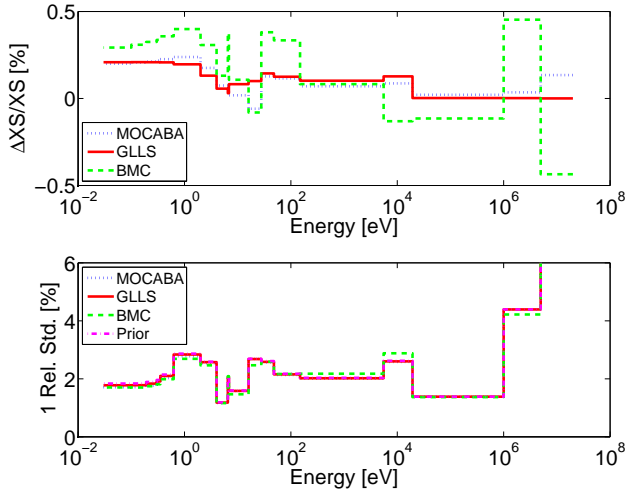

Fig. 4. Adjustments with each DA method to $^{238}U/\sigma_c$ as $\Delta XS/XS$ (above) and relative standard deviations (below).

Fig. 5 presents adjustments for $^{235}U/\sigma_f$. Again, strong agreement (within 0.01%) is seen between the adjusted cross sections and the posterior uncertainties for MOCABA and GLLS. The BMC method predicts larger adjustments to the cross section's data and larger reductions in its posterior uncertainty. In general, the posterior data with each method agree well and follow similar trends.

In conclusion, when examining these nuclear data, no clear trends can be seen concerning the DA methods' abilities to adjust nuclear data. In general, MOCABA and GLLS agree best, with larger disagreements between BMC and the MO-CABA/GLLS. These results do not provide any evidence to indicate that the non-linearities in the BHO samples created significant effects in the GLLS adjustments to nuclear data. Furthermore they provide evidence to support the hypothesis that the DA methods should be equivalent given linear integral parameters. Strong and definitive conclusions about the posterior nuclear data are harder to make concerning the working hypotheis. This is because the resonance self-shielding treatment in CASMO is not fully taken into account when the nuclear data are perturbed in SHARK-X.

3. H$_2$O: Adjustments to Calculated Values

The results from the data assimilation for the H$_2$O-moderated integral parameters are presented in Table II. First seen are the lower R^2 values for these $\Delta\rho_{rel}$ responses in com-
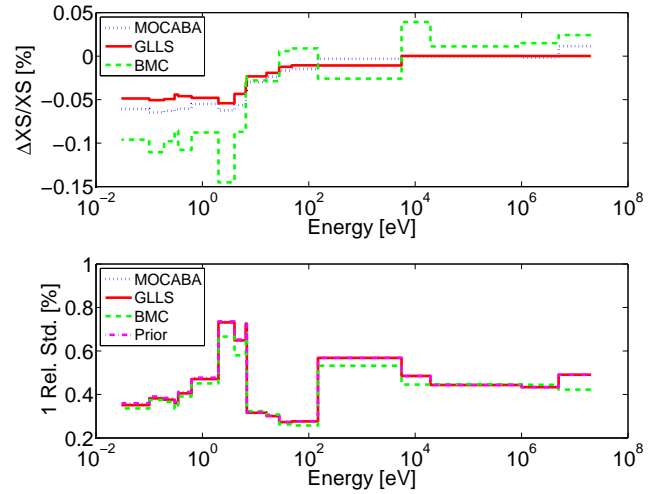

Fig. 5. Adjustments with each DA method to $^{235}U/\sigma_f$ as $\Delta XS/XS$ (above) and relative standard deviations (below).

parison to those moderated by BHO, especially for the UO$_2$ samples which have an average R^2 of 0.870. The possible effect of the higher degree of non-linearity can then be seen in the comparison of GLLS to MOCABA/BMC: both the posterior C'/Es and posterior relative standard deviations do not show the strong agreement between methods seen in Table I for BHO. Beginning with the UO$_2$ samples' posterior C'/E values, the average relative difference between GLLS' and MOCABA/BMC's C'/E values is approximately 0.9%. In contrast, the UO$_2$ samples' C'/E values for BHO, with an average R^2 of 0.975, have an average relative difference of less than 0.05% (much smaller than the posterior relative standard deviations) and smaller than the number of significant digits included in the experimental data.

Next the C'/Es for MOX samples' have an average R^2 of 0.964 and the average relative difference between C'/E values is ~1.2%. The identical MOX samples moderated by BHO, which have an average R^2 of 0.979, have an average relative difference between C'/E values of ~0.1%. The larger differences seen for the H$_2$O samples between the deterministic GLLS method and the stochastic MOCABA/BMC methods provides evidence to support the hypothesis that non-linearities in responses may exceed the limits of GLLS' linearity assumption.

Examining the posterior relative standard deviations calculated with each method, good agreement is seen between MOCABA and BMC but poor agreement between MO-CABA/BMC and GLLS. In fact, the GLLS uncertainties are approximately twice as large as those of MOCABA/BMC despite there being good agreement between the prior EGPT and SS relative standard deviations. In comparison to the posterior relative standard deviations shown in Table I for BHO, the discrepancies between GLLS and the stochastic methods are much greater for H$_2$O than BHO. This again provides evidence to support the hypothesis that non-linear responses like $\Delta\rho_{rel}$ limit the applicability of GLLS' theory and create discrepancies between GLLS' results and those of MOCABA

| Sample & | R^2 | Prior | Posterior Bias C'/E | | | Prior 1 Rel. Std. [%] | | Posterior 1 Rel. Std. [%] | | |
Burnup [MWd/kg]		C/E	GLLS	MOCABA	BMC	EGPT	SS ± Conf. Int.	GLLS	MOCABA	BMC
U1* (~40)	0.845	0.926	0.939	0.948	0.949	2.15	1.95 ± 0.09	1.39	0.54	0.53
U2 (~50)	0.848	0.983	0.994	1.002	1.002	1.64	1.48 ± 0.07	1.08	0.45	0.43
U3* (~70)	0.851	0.949	0.958	0.967	0.965	1.41	1.40 ± 0.06	0.99	0.46	0.44
U4* (~70)	0.893	0.944	0.953	0.962	0.960	1.42	1.42 ± 0.06	0.97	0.47	0.44
U5 (~90)	0.871	0.962	0.971	0.980	0.978	1.36	1.36 ± 0.06	0.96	0.48	0.46
U6 (~90)	0.879	0.964	0.973	0.981	0.980	1.34	1.36 ± 0.06	0.94	0.48	0.45
U7 (~120)	0.868	0.998	1.007	1.017	1.015	1.41	1.41 ± 0.06	1.00	0.51	0.47
UO_2 mean	0.870	0.962	0.972	0.981	0.980	1.53	1.48 ± 0.07	1.05	0.48	0.46
M1 (~20)	0.978	0.964	0.995	1.010	1.011	4.59	4.48 ± 0.20	2.70	1.13	1.19
M2 (~40)	0.967	0.953	0.974	0.987	0.987	3.11	3.02 ± 0.13	1.83	0.70	0.67
M3 (~60)	0.961	0.969	0.985	0.997	0.996	2.34	2.33 ± 0.10	1.47	0.62	0.56
M4* (~70)	0.950	1.013	1.028	1.040	1.039	2.08	2.09 ± 0.09	1.34	0.61	0.55
MOX mean	0.964	0.975	0.996	1.008	1.008	3.03	2.98 ± 0.13	1.83	0.77	0.74

TABLE II. Prior and posterior biases and 1-relative-standard deviations using each DA method for H_2O. An asterisk (*) indicates removal from influencing the adjustments by $\Delta\chi^2$-filtering.

and BMC.

To further analyze the results, the metamodeling was again used for these H_2O-moderated samples. The results of the metamodel analysis assess the uncertainty in the posterior values of MOCABA and BMC. This uncertainty is caused by using a finite sample size of 1,000 samples when estimating the prior distributions' moments that are inputs into the methods. This study seeks to eliminate the possibility of a Type I error in assessing the hypothesis. Here, the erroneous conclusion could be made that the differences seen are created by non-linearity and therefore support the hypothesis, whereas, in fact, they result only from statistical fluctuations.

The results of this metamodel analysis show that the uncertainties on the C'/E values of MOCABA and BMC (with standard deviations of 2E-4 to 9E-4) are not sufficiently large to account for the differences between the GLLS C'/Es. This indicates that it is unlikely that the discrepancies in Table II were caused by statistics and further supports the conclusion that they were caused by non-linearities. Additionally, the uncertainties of MOCABA and BMC C'/Es and relative standard deviations are sufficiently large to account for the disagreements seen between their results in Table II. This helps to confirm that these two methods are well formulated and consistent given identical input data.

4. H_2O: Adjustments to Nuclear Data

The comparison of each method's ability to adjust nuclear data with the H_2O moderator is summarized here by again focusing on $^{239}Pu/\bar{\nu}$, $^{238}U/\sigma_c$, $^{235}U/\sigma_f$ in Fig. 6, Fig. 7, and Fig. 8 respectively. Turning first to Fig. 6, good agreement is seen between all the methods in terms of $\Delta XS/XS$ and posterior relative uncertainties. While the size and direction of the adjustments are different for the H_2O moderator in comparison to the BHO moderator, the behavior and trends are consistent between these sets of integral parameters. This

shows that for this nuclide/reaction pair, the H_2O-moderated responses' higher degrees of non-linearity did not introduce major inconsistencies.
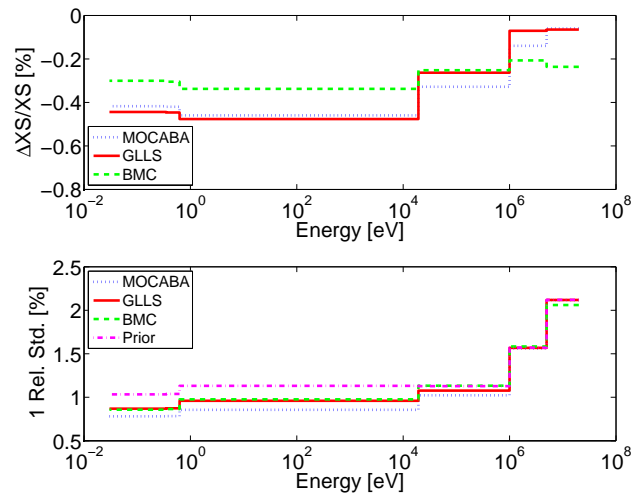

Fig. 6. Adjustments with each DA method to $^{239}Pu/\bar{\nu}$ as $\Delta XS/XS$ (above) and relative standard deviations (below).

Fig. 7 presents the adjustments for $^{238}U/\sigma_c$. Here, discrepancies between the stochastic MOCABA/BMC methods and GLLS appear. At thermal energies, BMC adjusts the data by 1.9-2.2% and MOCABA by 1.5-1.8%. GLLS, in contrast, creates adjustments of 0.6-0.7%. Higher energies also show the same dynamic of closer agreement between the stochastic methods than with GLLS. This may provide evidence that the non-linearities in the H_2O-moderated responses do have an effect in the GLLS method which can lead to disagreements between its results and those of MOCABA or BMC.
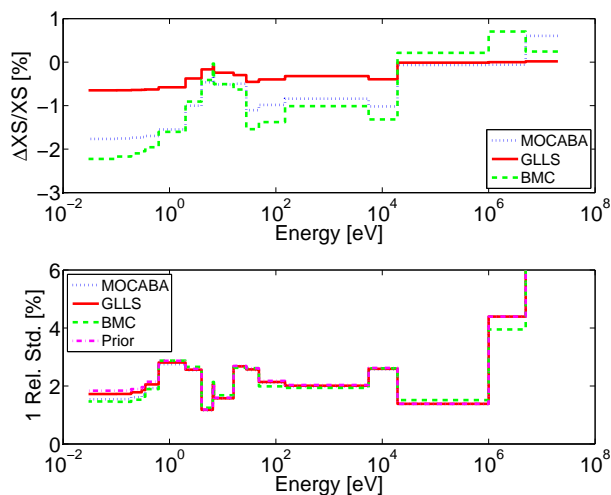
Fig. 7. Adjustments with each DA method to $^{238}U/\sigma_c$ as ΔXS/XS (above) and relative standard deviations (below).

The adjustments for $^{235}U/\sigma_f$ are presented in Fig. 8. Strong agreement is seen in the thermal energy range between MOCABA and GLLS. The BMC method creates adjustments that are inconsistent with MOCABA and GLLS in the thermal range, where the adjustments are two to three times as large. Additionally for BMC, similar behavior to what was seen in Fig. 5 concerning the posterior uncertainties appears in the energy group from 1.5E2 eV to 5.5E4 eV: the posterior uncertainties are larger than the priors. Again, strong agreement (within 0.01%) is seen between the adjusted cross sections and the posterior uncertainties for MOCABA and GLLS. The BMC method predicts larger adjustments to the cross section's data and larger reductions in its posterior uncertainty. In general, the posterior data with each method agree well and follow similar trends.
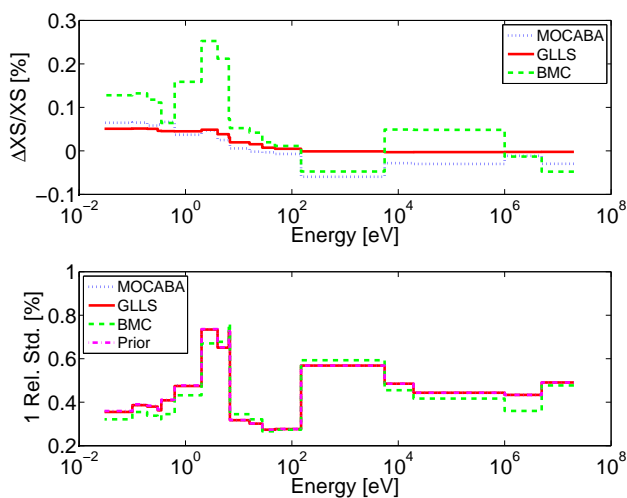

Fig. 8. Adjustments with each DA method to $^{235}U/\sigma_f$ as ΔXS/XS (above) and relative standard deviations (below).

In conclusion when examining these nuclear data, no clear trends can be seen concerning the DA methods' abilities to adjust nuclear data. In Fig. 6, the methods produce consistent and comparable adjustments. In contrast, Fig. 7 shows stronger agreement between MOCABA and BMC and weaker agreement between those two methods and GLLS. This behavior tends to support the hypothesis that the stochastic methods would agree well when non-linearities are present and be demonstrably different from GLLS. Finally, in Fig. 8, stronger agreement is shown between MOCABA and GLLS with BMC providing inconsistent adjustments. These results lead to the conclusion that the non-linearities may have an effect on the GLLS adjustments to nuclear data, but they cannot be proven within the case study presented here. In a global sense, the methods agree well and all adjustments are within their 1-relative-standard deviations, criteria used in [1] to assess the agreement between institution's adjustment results.

V. CONCLUSIONS

The comparison between GLLS, MOCABA, and BMC was performed for two moderating conditions that were present during the LWR-Proteus Phase II campaign: borated water (BHO) and pure water (H_2O). The H_2O-moderated integral parameters showed non-linear behavior and were used to assess if non-linearities would have a significant impact on the GLLS methodology's results, particularly the posterior calculated values and nuclear data. The BHO moderated responses, being fairly linear, served as a control to show that the stochastic methods would agree with GLLS given the linearity assumption was accurate. The results of the case study provided evidence to support the hypothesis that the methods would agree well for linear integral parameters, but that non-linearities can cause significant discrepancies between the stochastic methods and GLLS.

First, the posteriors with the three methods for the BHO moderated responses showed strong agreement in C/E, with their values never differing by greater than 0.2%. The posterior uncertainties showed some small but statistically significant disagreement between MOCABA/BMC and GLLS. This led to the general conclusion that the methods were well formulated and agree well for linear responses. The examination of the posterior nuclear data did not show any significant disagreement between the methods. The BMC method showed behavior most inconsistent with the other methods, especially at thermal energies for $^{238}U/\sigma_c$ and $^{235}U/\sigma_f$. Continuing to the H_2O moderated responses, statistically significant disagreements were then found between GLLS results and those of BMC and MOCABA. These disagreements were especially large in the posterior uncertainties of the calculated responses, where differences of 0.5-1.0% were calculated. These differences supported the hypothesis that these non-linearities would affect the GLLS method's results. The comparison of the posterior nuclear data for these responses was inconclusive concerning the effect of non-linearities in the integral parameters on the GLLS method's adjustments to nuclear data.

The results are auspicious for the ultimate goal of the project: to use SHARK-X to perform DA to reduce the bias and bias uncertainty of a hypothetical spent fuel pool of a

Swiss nuclear power plant with LWR-Proteus Phase II results. The results show that the three methods are well formulated and have been well integrated into the SHARK-X tool. The effect of non-linearities in the responses will need to be closely considered when using the experimental data set for this application and when interpreting the results.

VI. ACKNOWLEDGMENTS

REFERENCES

1. M. SALVATORES ET AL., "Methods and Issues for the Combined Use of Integral Experiments and Covariance Data: Results of a NEA International Collaborative Study," *Nuclear Data Sheets*, **118** (2014).
2. DRAGT, "Statistical Considerations on Techniques for Adjustment of Differential Cross Section with Measured Integral Parameters," Tech. rep. (1970).
3. B. HOEFER ET AL., "MOCABA: A general Monte Carlo-Bayes procedure for improved predictions of integral functions of nuclear data," *Annals Nuclear Energy*, **77** (2015).
4. A. KONING, "The Bayesian Monte Carlo Method for Nuclear Data Evaluation," *The European Physical Journal A*, **51** (2015).
5. E. ALHASSAN ET AL., "On the use of integral experiments for uncertainty reduction of reactor macroscopic parameters within the TMC methodology," *Progress in Nuclear Energy*, **88** (2016).
6. P. GRIMM ET AL., "CASMO-5 Analysis of Reactivity Worths of Burnt PWR Fuel Samples Measured in LWR-PROTEUS Phase II," in "PHYSOR 2016 - Unifying Theory and Experiments in the 21st Century," (2016).
7. J. RHODES ET AL., "CASMO-5 User's Manual Rev. 5." **SSP-07/431** (2012).
8. W. WIESELQUIST ET AL., "PSI Methodologies for Nuclear Data Uncertainty Propagation with CASMO-5M and MCNPX: Results for OECD/NEA UAM Benchmark Phase I," *Science and Technology of Nuclear Installations* (2013).
9. M. L. WILLIAMS and B. T. REARDEN, "SCALE-6 Sensitivity/Uncertainty Methods and Covariance Data," *Nuclear Data Sheets*, **109** (2008).
10. M. DEGROOTN and M. SCHERVISH, *Probability and Statistics*, Addison-Wesley, 4 ed. (2012).
11. M. L. WILLIAMS ET AL., "6.6 TSURFER: An Adjustment Code to Determine Biases and Uncertainties in Nuclear System Responses by Consolidating Differential Data and Benchmark Integral Experiments," *SCALE: A Comprehensive Modeling and Simulation Suite for Nuclear Safety Analysis and Design, ORNL/TM-2005/39, Version 6.1* (2011).